

BIFURCATIONS IN AN AUTOPARAMETRIC SYSTEM IN 1:1 INTERNAL RESONANCE WITH PARAMETRIC EXCITATION

(revised preprint nr. 1129)

S. Fatimah*, and M. Ruijgrok

*Mathematisch Instituut, University of Utrecht, PO Box 80.010, 3508 TA Utrecht,
The Netherlands*

ABSTRACT. We consider an autoparametric system which consists of an oscillator, coupled with a parametrically-excited subsystem. The oscillator and the subsystem are in 1 : 1 internal resonance. The excited subsystem is in 1 : 2 parametric resonance with the external forcing. The system contains the most general type of cubic nonlinearities. Using the method of averaging and numerical bifurcation continuation, we study the dynamics of this system. In particular, we consider the stability of the semi-trivial solutions, where the oscillator is at rest and the excited subsystem performs a periodic motion. We find various types of bifurcations, leading to non-trivial periodic or quasi-periodic solutions. We also find numerically sequences of period-doublings, leading to chaotic solutions.

1. INTRODUCTION

An autoparametric system is a vibrating system which consists of at least two subsystems: the oscillator and the excited subsystem. This system is governed by differential equations where the equations representing the oscillator are coupled to those representing the excited subsystem in a nonlinear way and such that the excited subsystem can be at rest while the oscillator is vibrating. We call this solution the semi-trivial solution. When this semi-trivial solution becomes unstable, non-trivial solutions can be initiated. For more backgrounds and references see Svoboda, Tondl, and Verhulst [1] and Tondl, Ruijgrok, Verhulst, and Nabergoj [2].

We shall consider an autoparametric system where the oscillator is excited parametrically, of the form:

$$(1.1) \quad \begin{aligned} x'' + k_1 x' + q_1^2 x + ap(\tau)x + f(x, y) &= 0 \\ y'' + k_2 y' + q_2^2 y + g(x, y) &= 0 \end{aligned}$$

The first equation represents the oscillator and the second one is the excited subsystem. An accent, as in x' , will indicate differentiation with

*corresponding author

respect to time τ and $x, y \in \mathbb{R}$. k_1 and k_2 are the damping coefficients, q_1 and q_2 are the natural frequencies of the undamped, linearized oscillator and excited subsystem, respectively. The functions $f(x, y)$ and $g(x, y)$, the coupling terms, are C^∞ and $g(x, 0) = 0$ for all $x \in \mathbb{R}$. The damping coefficients and the amplitude of forcing a are assumed to be small positive numbers. We will consider the situation that the oscillator and the external parametric excitation are in primary 1 : 2 resonance and that there exists an internal 1 : 1 resonance.

There exist a large number of studies of similar autoparametric systems. The case of a 1 : 2 internal resonance has been studied by Ruijgrok [3] and Oueini, Chin, and Nayfeh [4], in the case of parametric excitation. In Ruijgrok [3] the averaged system is analyzed mathematically, and an application to a rotor system is given. In Oueni, Chin, and Nayfeh [4] theoretical results are compared with the outcomes of a mechanical experiment. Tien, Namachchivaya, and Bajaj [5] also consider the situation that there exists a 1 : 2 internal resonance, now however with external excitation.

In Tien, Namachchivaya, and Bajaj [5] and in Bajaj, Chang and Johnson [6] the bifurcations of the averaged system are studied, and the authors show the existence of chaotic solutions, numerically in Bajaj, Chang, and Johnson [6] and by using an extension of the Melnikov method in Tien, Namachchivaya, and Bajaj [5], for the case with no damping. In Banerjee and Bajaj [7], similar methods as in Tien, Namachchivaya, and Bajaj [5] are used, but now for general types of excitation, including parametric excitation.

The case of a 1 : 1 internal resonance has received less attention. In Tien, Namachchivaya, and Malhotra [8] this resonance case is studied, in combination with external excitation. The author shows analytically that for certain values of the parameters, a Šilnikov bifurcation can occur, leading to chaotic solutions. In Feng and Sethna [9] parametric excitation was considered, and also here a generalization of the Melnikov method was used to show the existence of chaos in the undamped case.

In this paper we study the behavior of the semi-trivial solution of system (1.1). This is done by using the method of averaging. It is found that several semi-trivial solutions can co-exist. These semi-trivial solutions come in pairs, connected by a mirror-symmetry. However, only one of these (pairs of) semi-trivial solutions is potentially stable. In section 4 we study the stability of this particular solution, the results of which are summarized in 3-dimensional stability diagrams. In section 5 the bifurcations of the semi-trivial solution are analyzed. These bifurcations lead to non-trivial solutions, such as stable periodic and quasi-periodic orbits. In section 6 we show that one of the non-trivial solutions undergoes a series of period-doublings, leading to a strange attractor. The chaotic nature of this attractor is demonstrated by calculating the associated Lyapunov exponents.

Finally, we mention that in the averaged system we encounter a codimension 2 bifurcation. The study of this rather complicated bifurcation will

be described in a separate paper, where we also use a method similar to the one used in Tien, Namachchivaya, Malhotra [8] to show analytically the existence of Šilnikov bifurcations in this system.

2. THE AVERAGED SYSTEM

We will take $f(x, y) = c_1xy^2 + \frac{4}{3}x^3$, $g(x, y) = \frac{4}{3}y^3 + c_2x^2y$, and $p(\tau) = \cos 2\tau$. Let $q_1^2 = 1 + \epsilon\sigma_1$ and $q_2^2 = 1 + \epsilon\sigma_2$, where σ_1 and σ_2 are the detunings from exact resonance. After rescaling $k_1 = \epsilon\tilde{k}_1$, $k_2 = \epsilon\tilde{k}_2$, $a = \epsilon\tilde{a}$, $x = \sqrt{\epsilon}\tilde{x}$, and $y = \sqrt{\epsilon}\tilde{y}$, then dropping the tildes, we have the system:

$$(2.1) \quad \begin{aligned} x'' + x + \epsilon(k_1x' + \sigma_1x + a \cos 2\tau x + \frac{4}{3}x^3 + c_1y^2x) &= 0 \\ y'' + y + \epsilon(k_2y' + \sigma_2y + c_2x^2y + \frac{4}{3}y^3) &= 0 \end{aligned}$$

It is possible to start with a more general expression for $f(x, y)$ and $g(x, y)$, for instance including quadratic terms. We have limited ourselves to the lowest-order resonant terms, which in this case are of third order, and which can be put in this particular form by a suitable scaling of the x , y , and τ -coordinates. This is not a restriction, as a more general form for the coupling terms leads to the same averaged system and normal forms.

The system (2.1) is invariant under $(x, y) \rightarrow (x, -y)$, $(x, y) \rightarrow (-x, y)$, and $(x, y) \rightarrow (-x, -y)$. In particular the first symmetry will be important in the analysis of this system. We emphasize that these symmetries do not depend on our particular choice for $f(x, y)$ and $g(x, y)$, but are a consequence of the 1:2 and 1:1 resonances and the restriction that we have an autoparametric system, i.e. that $g(x, 0) = 0$ for all $x \in \mathbb{R}$.

We will use the method of averaging (see Sanders and Verhulst [10] for appropriate theorems) to investigate the stability of solutions of system (2.1), by introducing the transformation:

$$(2.2) \quad x = u_1 \cos \tau + v_1 \sin \tau \quad ; \quad x' = -u_1 \sin \tau + v_1 \cos \tau$$

$$(2.3) \quad y = u_2 \cos \tau + v_2 \sin \tau \quad ; \quad y' = -u_2 \sin \tau + v_2 \cos \tau$$

After substituting (2.2) and (2.3) into (2.1), averaging over τ , and rescaling $\tau = \frac{\epsilon}{2}\tilde{\tau}$, we have the following averaged system:

$$\begin{aligned}
(2.4) \quad & u_1' = -k_1 u_1 + \left(\sigma_1 - \frac{1}{2}a\right)v_1 + v_1(u_1^2 + v_1^2) + \frac{1}{4}c_1 u_2^2 v_1 + \frac{3}{4}c_1 v_2^2 v_1 + \frac{1}{2}c_1 u_2 v_2 u_1 \\
& v_1' = -k_1 v_1 - \left(\sigma_1 + \frac{1}{2}a\right)u_1 - u_1(u_1^2 + v_1^2) - \frac{3}{4}c_1 u_2^2 u_1 - \frac{1}{4}c_1 v_2^2 u_1 - \frac{1}{2}c_1 u_2 v_2 v_1 \\
& u_2' = -k_2 u_2 + \sigma_2 v_2 + v_2(u_2^2 + v_2^2) + \frac{1}{4}c_2 u_1^2 v_2 + \frac{3}{4}c_2 v_1^2 v_2 + \frac{1}{2}c_2 u_1 v_1 u_2 \\
& v_2' = -k_2 v_2 - \sigma_2 u_2 - u_2(u_2^2 + v_2^2) - \frac{3}{4}c_2 u_1^2 u_2 - \frac{1}{4}c_2 v_1^2 u_2 - \frac{1}{2}c_2 u_1 v_1 v_2
\end{aligned}$$

3. THE SEMI-TRIVIAL SOLUTION

In this section we investigate the semi-trivial solutions of system (2.4) and determine their stability. From section 1, the semi-trivial solutions correspond to $u_2 = v_2 = 0$, so that we have:

$$\begin{aligned}
(3.1) \quad & u_1' = -k_1 u_1 + \left(\sigma_1 - \frac{1}{2}a\right)v_1 + v_1(u_1^2 + v_1^2) \\
& v_1' = -k_1 v_1 - \left(\sigma_1 + \frac{1}{2}a\right)u_1 - u_1(u_1^2 + v_1^2)
\end{aligned}$$

Apart from $(0, 0)$, the fixed points of system (3.1) correspond with periodic solutions of system (2.1). The non-trivial fixed points are

$$(3.2) \quad (\pm u_o, \pm v_o) = \left(\pm \frac{R_o k_1^2}{-(\sigma_1 + \frac{1}{2}a + R_o^2) \sqrt{(\sigma_1 - \frac{1}{2}a + R_o^2)^2 + k_1^2}}, \pm \frac{R_o k_1}{\sqrt{(\sigma_1 - \frac{1}{2}a + R_o^2)^2 + k_1^2}} \right)$$

where

$$(3.3) \quad R_o^2 = -\sigma_1 \pm \sqrt{\frac{1}{4}a^2 - k_1^2}$$

Assuming $R_o \neq 0$, there are three cases, depending on the value of a and σ_1

1. If $a > 2\sqrt{\sigma_1^2 + k_1^2}$, there is one solution for R_o^2
2. If $\sigma_1 < 0$ and $2k_1 < a < 2\sqrt{\sigma_1^2 + k_1^2}$, there are two solutions for R_o^2
3. For $a < 2k_1$, there is no solution for R_o^2 .

These results are summarized in Figure 1. The phase-portraits of system (3.1) in the (u_1, v_1) -plane for a specific value (σ_1, a) in these regions are indicated in Figure 2. Note that the fixed-points come in pairs and are symmetric with respect to $(0, 0)$.

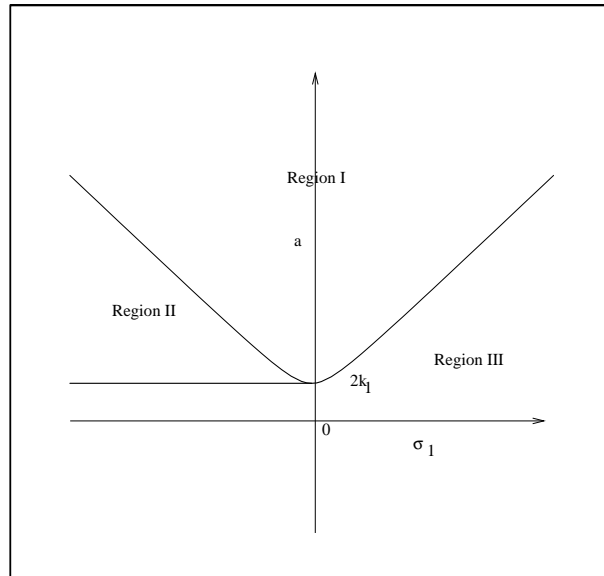


FIGURE 1. The parameter diagram of system (3.1) in the (σ_1, a) -plane

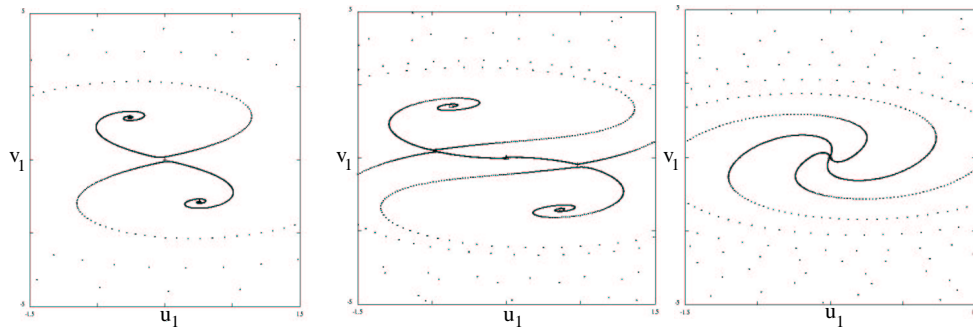


FIGURE 2. The phase-portraits of system (3.1) in the (u_1, v_1) -plane for specific values (σ_1, a) in region I, II, and III, respectively.

4. STABILITY OF THE SEMI-TRIVIAL SOLUTION

In this section we will study the stability of the semi-trivial solution depending on the values of the forcing amplitude a and the detunings σ_1, σ_2 in system (2.1). From section 3, we find that the semi-trivial solution corresponding to R_o^2 with the plus sign is always stable (as a solution of (3.1)), therefore we will only study this semi-trivial solution and ignore the unstable semi-trivial solutions.

Write the averaged system (2.4) in the form:

$$(4.1) \quad \mathbf{X}' = F(\mathbf{X})$$

where $\mathbf{X} = \begin{pmatrix} u_1 \\ v_1 \\ u_2 \\ v_2 \end{pmatrix}$ and

$$(4.2) \quad \frac{\partial F}{\partial \mathbf{X}} = \begin{pmatrix} A_{11} & A_{12} \\ A_{21} & A_{22} \end{pmatrix}$$

where A_{11} , A_{12} , A_{21} , and A_{22} are 2×2 matrices depending on u_1 , v_1 , u_2 and v_2 . At the solution $(\pm u_o, \pm v_o, 0, 0)$, corresponding to the semi-trivial solution of system (4.1), we have $\frac{\partial F}{\partial \mathbf{X}} = A\mathbf{X}$ with

$$(4.3) \quad A = \begin{pmatrix} -k_1 + 2u_o v_o & \sigma_1 - \frac{1}{2}a + 2v_o^2 + R_o^2 & 0 & 0 \\ -\sigma_1 - \frac{1}{2}a - 2u_o^2 - R_o^2 & -k_1 - 2u_o v_o & 0 & 0 \\ 0 & 0 & -k_2 + \frac{1}{2}c_2 u_o v_o & \sigma_2 + \frac{1}{4}c_2 u_o^2 + \frac{3}{4}c_2 v_o^2 \\ 0 & 0 & -\sigma_2 - \frac{1}{4}c_2 v_o^2 - \frac{3}{4}c_2 u_o^2 & -k_2 - \frac{1}{2}c_2 u_o v_o \end{pmatrix}$$

u_o and v_o satisfy (3.4) and R_o^2 satisfies (3.6). Let

$$A = \begin{pmatrix} A_{11} & 0 \\ 0 & A_{22} \end{pmatrix}$$

To get the stability boundary of system (4.1), we solve $\det A = \det A_{11} \det A_{22} = 0$. From the equation $\det A_{11} = 0$ we find

$$2(\sqrt{\frac{1}{4}a^2 - k_1^2})(\sqrt{\frac{1}{4}a^2 - k_1^2} - \sigma_1) = 0$$

or

$$(4.4) \quad a = 2k_1 \quad \text{or} \quad a = 2\sqrt{\sigma_1^2 + k_1^2}$$

and from $\det A_{22} = 0$, we have:

$$(4.5) \quad \sigma_2 = -\frac{1}{2}c_2 R_o^2 \pm \sqrt{\frac{1}{16}c_2^2 R_o^4 - k_2^2} \quad \text{where} \quad R_o^2 \geq 4\frac{k_2}{c_2}$$

Because R_o^2 is a function of σ_1 and a , equation (4.5) now gives a relation between σ_1 , σ_2 , and a . Graphically, this corresponds to a surface in the 3-dimensional parameter space (σ_1, a, σ_2) . This surface is shown in Figure 3 for fixed values of $k_1, k_2, c_1, c_2 > 0$ and in Figure 4 for fixed values of $k_1, k_2, c_1 > 0$ and $c_2 < 0$.

In figure 5 we show the stability boundary in the (σ_1, σ_2) -plane for a fixed value of $a > 2k_1$. Inside the curve the semi-trivial solution is unstable, outside it is stable. In these numeric calculations we fixed $k_1 = 1, k_2 = 1$ and $c_1 = 1$. We took $c_2 = 1$, for the case $c_2 > 0$ and $c_2 = -1$ for the case $c_2 < 0$.

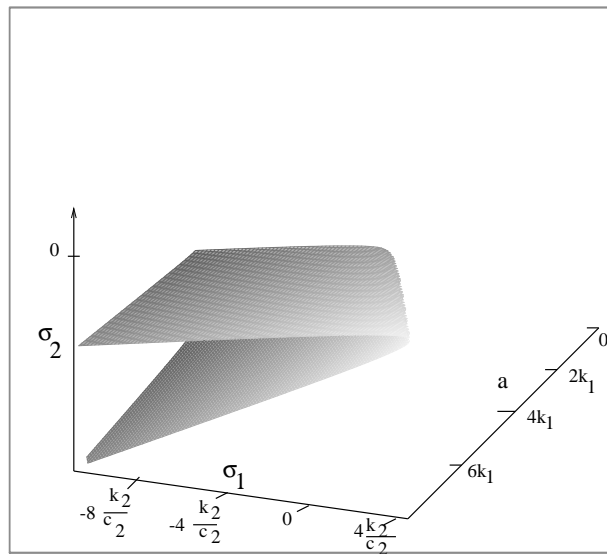


FIGURE 3. The parameter-space of system (4.1) in the (a, σ_1, σ_2) -space for $c_2 > 0$.

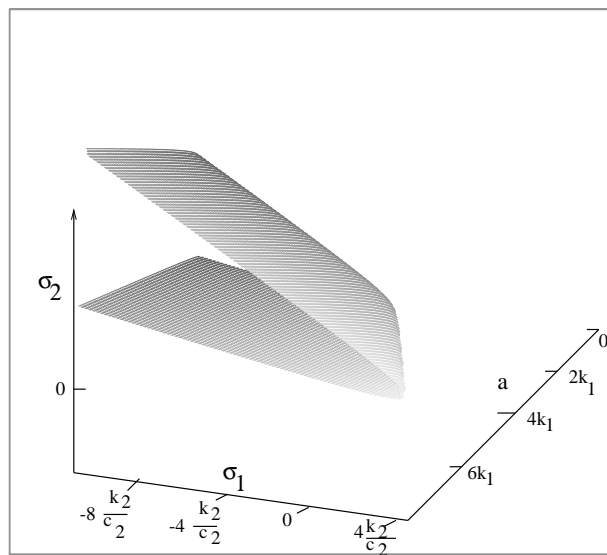


FIGURE 4. The parameter-space of system (4.1) in the (a, σ_1, σ_2) -space for $c_2 < 0$.

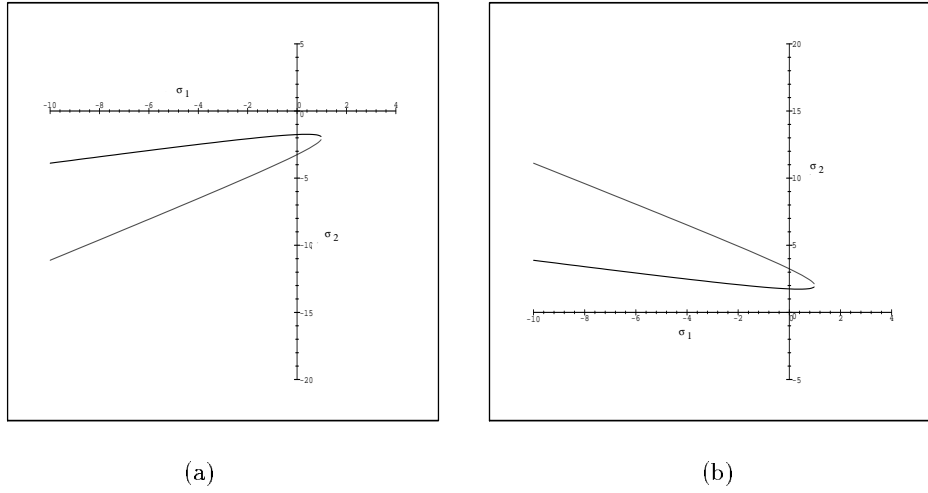


FIGURE 5. The parameter diagram of system (4.1) in the (σ_1, σ_2) -plane for fixed $a = 10.20$. In figure (a) for $c_2 > 0$ and in figure (b) for $c_2 < 0$.

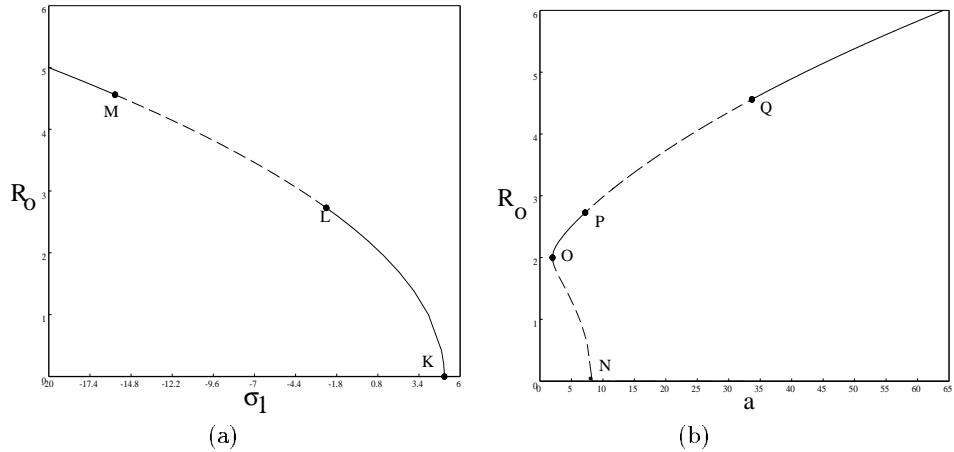


FIGURE 6. The stability diagram of the response of system (4.1), (a) against the detuning σ_1 for fixed $a = 10.2$ and $\sigma_2 = -5.3$ and (b) against the forcing a for fixed $\sigma_1 = -4$ and $\sigma_2 = -5.3$. A solid line means that the semi-trivial solution is stable and the dashed line that it is unstable.

In Figure 6 (a) we show the response of $R_1^2 = u_1^2 + v_1^2$ for fixed a and σ_2 , note that $R_o = R_1$. We find that between the branch points L and M the semi-trivial solution is unstable. In Figure 6 (b) we show the response R_o for fixed σ_1 and σ_2 . We have indicated that the semi-trivial solution is unstable between the branch points N and O, and between the branch points P and

Q. Figure 6 does not depend on the sign of c_2 . We have similar figures for the case $c_2 > 0$, $\sigma_2 < 0$ and for the case $c_2 < 0$, $\sigma_2 > 0$.

5. BIFURCATIONS OF THE SEMI-TRIVIAL SOLUTION

On the stability boundary shown in Figure 3, the semi-trivial solution undergoes a pitchfork bifurcation. We have used the bifurcation continuation program CONTENT (Kuznetsov [11]) to study the non-trivial solutions branching from these bifurcation points. We find that the results depend on the values of c_1 and c_2 . For positive values of c_1 and c_2 , the results are summarized in Figure 7.

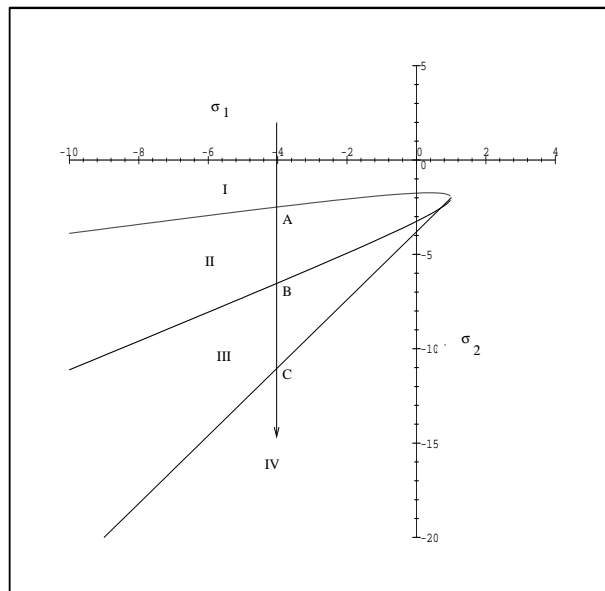


FIGURE 7. The parameter diagram of system (4.1) in the (σ_1, σ_2) plane for $c_2 > 0$.

We have fixed $a > 2k_1$ for values (σ_1, σ_2) in Region I, where the semi-trivial solution is stable. Crossing the boundary from Region I into Region II it becomes unstable and an attracting non-trivial solution is born. Crossing the boundary from Region II into III the semi-trivial solution becomes stable and a small, unstable non-trivial solution appears. Crossing the boundary from Region III into region IV the stable and unstable non-trivial solutions collide and disappear in a saddle-node bifurcation.

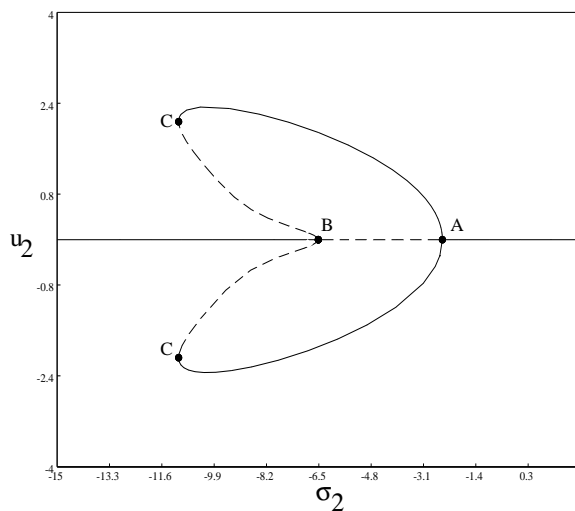


FIGURE 8. The bifurcation diagram of the semi-trivial solution in the (σ_2, u_2) -plane for $c_2 > 0$.

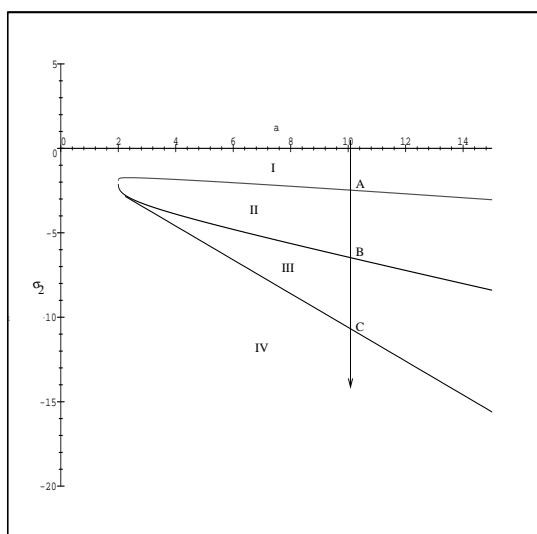


FIGURE 9. The parameter diagram of system (4.1) in the (a, σ_2) -plane, for $c_2 > 0$.

In Figure 8 we fix $a = 10.20$ and $\sigma_1 = -4$ (see Figure 7) and show the u_2 component of the non-trivial solution as σ_2 is varied. We have indicated the bifurcation points A, B, and C corresponding to Figure 7. There is an interval for σ_2 where two stable solutions coexist and on the boundaries of this interval hysteresis jumps occur.

It is possible to make similar diagrams in the (a, σ_2) -plane, keeping σ_1 fixed. Again we find similar bifurcations, see Figure 9. Note that the points A, B correspond to the branching points in Figure 8, and C corresponds to a saddle-node bifurcation.

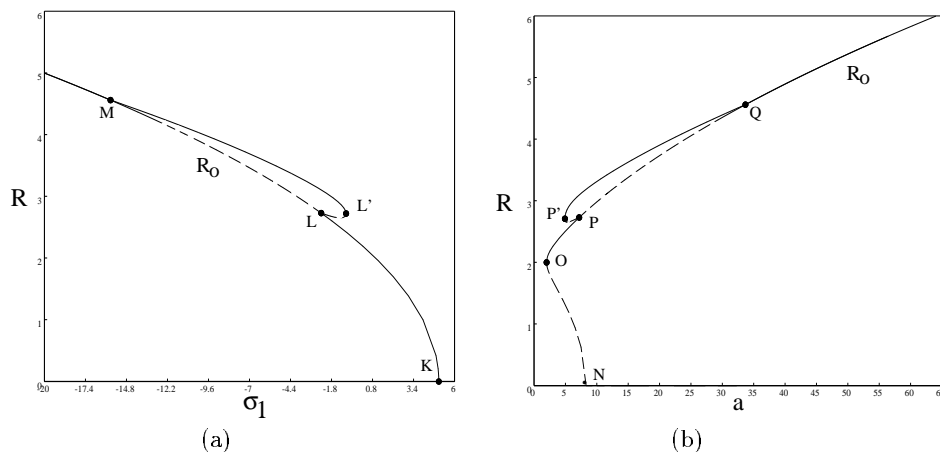


FIGURE 10. The stability diagram of the non-trivial solution R together with the response R_o of the semi-trivial solution for $c_2 > 0$, (a) against the detuning σ_1 for fixed $a = 10.2$ and $\sigma_2 = -5.3$ and (b) against the forcing a for fixed $\sigma_1 = -4$ and $\sigma_2 = -5.3$.

In Figure 10 (a) we show the amplitude of the non-trivial solution $R = \sqrt{u_1^2 + v_1^2 + u_2^2 + v_2^2}$, together with the amplitude of the semi-trivial solution for fixed a and σ_2 (see Figure 6(a)). We find two non-trivial solutions in certain interval of σ_1 . One is stable and another is unstable. We also show that between points L' and M the non-trivial solution is stable and there exists an unstable non-trivial solution between points L and L'. In Figure 10(b) we show the amplitude R , together with the amplitude of the semi-trivial solution R_o for fixed σ_1 and σ_2 (see Figure 6 (b)). The non-trivial solution is stable between points P' and Q and there exists an unstable non-trivial solution between points P and P'.

For negative values of c_2 we find different phenomena in the behavior of solutions of system (4.1). On the stability boundary shown in Figure 4, the semi-trivial solution undergoes a pitchfork bifurcation but then the non-trivial solutions which branches from this bifurcation point undergoes a Hopf bifurcation. Again we have used CONTENT to study the non-trivial solution branching from these bifurcation points. The results are illustrated in Figure 11.

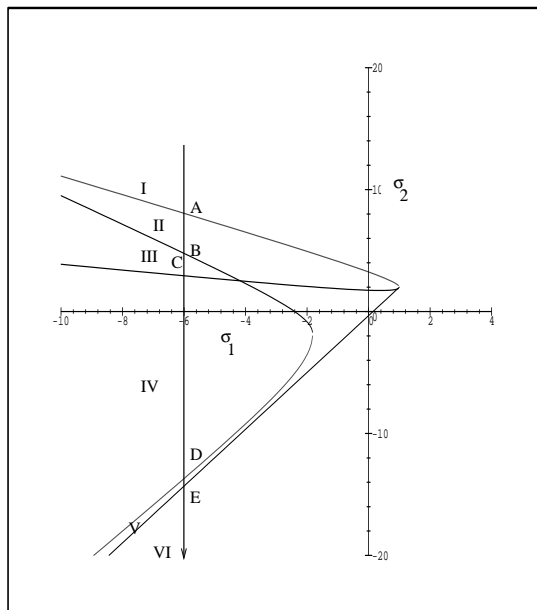


FIGURE 11. The parameter diagram of system (4.1) in the (σ_1, σ_2) -plane for $c_2 < 0$ and fixed $a = 10.20$.

We have fixed $a > 2k_1$ for values (σ_1, σ_2) in region I. In this region the semi-trivial solution is stable. Crossing the boundary from Region I into Region II it becomes unstable and a stable non-trivial solution appears. Crossing the boundary from Region II into III the non-trivial solution becomes unstable. A supercritical Hopf bifurcation occurs at the boundary between Region II and III. Crossing the boundary from Region III into IV the semi-trivial solution becomes stable and another small unstable non-trivial solution appears. Crossing the boundary from Region IV into V the unstable non-trivial solution changes its stability and again it undergoes a supercritical Hopf bifurcation. Finally, crossing the boundary V into VI the stable and unstable non-trivial solution collide and disappear in a saddle-node bifurcation.

In Figure 12 we fix $a = 10.2$ and $\sigma_1 = -6$ (see Figure 11) and show the v_2 component of the non-trivial solution as σ_2 is varied. We have indicated the bifurcation points A, B, C, D, and E corresponding to Figure 11. The points A and C indicate the branching points of the semi-trivial solution. The points B and D indicate Hopf bifurcation points and E a saddle-node bifurcation point. Again there is an interval for σ_2 where two stable solutions coexist and on the boundaries of this interval hysteresis jumps occur.

As we discussed in the case $c_2 > 0$, for $c_2 < 0$ we find similar bifurcations in the (a, σ_2) -plane (see Figure 13), keeping σ_1 fixed. The points A, B, C, D, and E on the curves correspond to the bifurcation points in Figure 12.

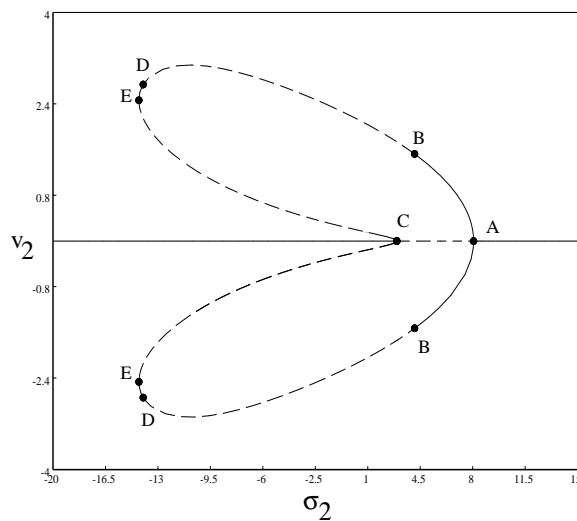


FIGURE 12. The stability diagram of system (4.1) in the (σ_2, v_2) -plane for $c_2 < 0$.

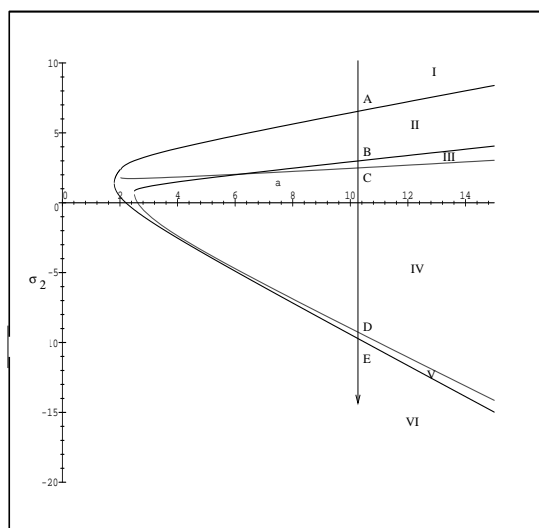


FIGURE 13. The parameter diagram of system (4.1) in the (a, σ_2) -plane for $c_2 < 0$

We note that the amplitude of the non-trivial solution of system (4.1) is $R = \sqrt{u_1^2 + v_1^2 + u_2^2 + v_2^2}$. In Figure 6 (a) we have depicted the amplitude of the semi-trivial solution R_o against σ_1 for fixed a and σ_2 . In Figure 14 (a), we show both the amplitude of the non-trivial solution R and the amplitude of semi-trivial solution R_o . When σ_1 is varied, we find there is an interval of σ_1 consisting of the unstable semi-trivial solution and the stable non-trivial solution. There is also interval of σ_1 where the semi-trivial solution is stable together with the stable non-trivial solution and the unstable non-trivial solution. In Figure 14 (b) we show the amplitude R , together with the amplitude R_o against a for fixed σ_1 and σ_2 . Again the same behavior of solutions of system (4.1) occurs, when a is varied.

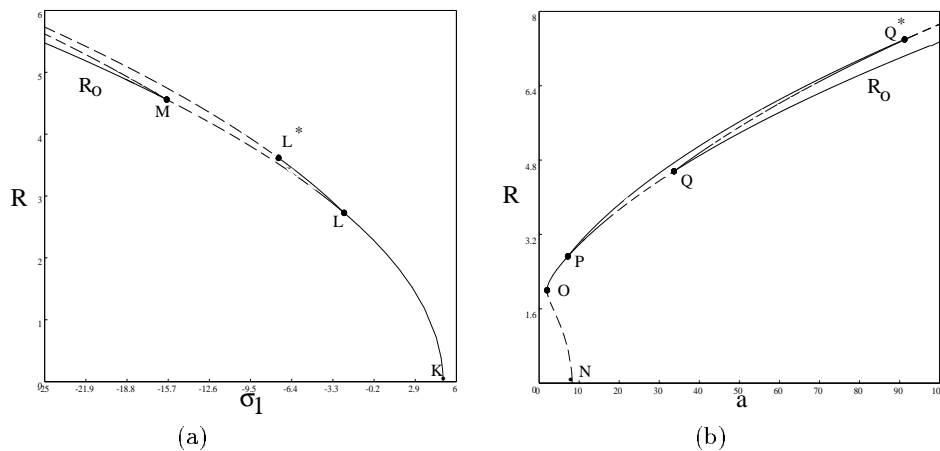


FIGURE 14. The stability diagram of the non-trivial solution R together with the semi-trivial solution for $c_2 < 0$, (a) against the detuning σ_1 for fixed $a = 10.2$ and $\sigma_2 = 5.3$ and (b) against the forcing a for fixed $\sigma_1 = -4$ and $\sigma_2 = 5.3$.

6. PERIOD DOUBLING BIFURCATIONS AND CHAOTIC SOLUTIONS

We now consider the case that $c_1 > 0$ and $c_2 < 0$. Not only does the system exhibit Hopf bifurcations, but we also observe a sequence of period-doublings, leading to a strange attractor.

In previous sections we have chosen a fixed value of a not too close to the stability boundary given by $a = 2k_1$. This was done because when a is in the neighbourhood of $2k_1$, complications can arise, since then also $\det A_{11} = 0$, and we can have double-zero eigenvalues. This problem can be studied analytically by considering a codimension 2 bifurcation; this will be carried out in a separate paper. As a first result from this bifurcation analysis we mention the occurrence of global bifurcations, involving heteroclinic and homoclinic loops. We also find a homoclinic solution of Šilnikov type. It is well-known (see Kuznetsov [11] and Wiggins [12]) that the existence of such a homoclinic loop is connected with chaotic solutions. We therefore

conjecture that the chaotic solutions we find numerically are the result of the Šilnikov phenomenon.

In the numeric calculations, presented in this section interesting behavior of solutions of system (4.1) occurs near the stability boundary.

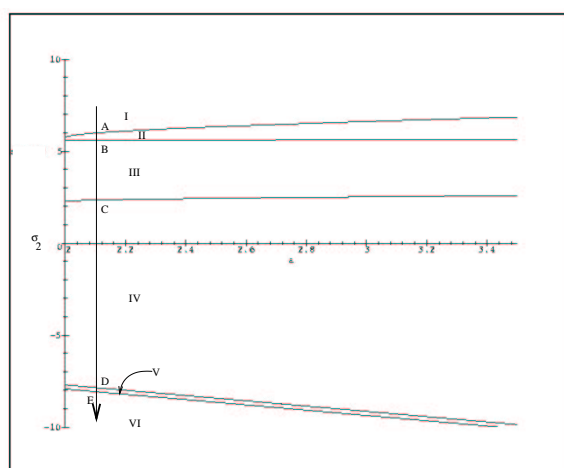


FIGURE 15. The parameter diagram of system (4.1) in the (a, σ_2) -plane for $c_2 < 0$ close to the stability boundary.

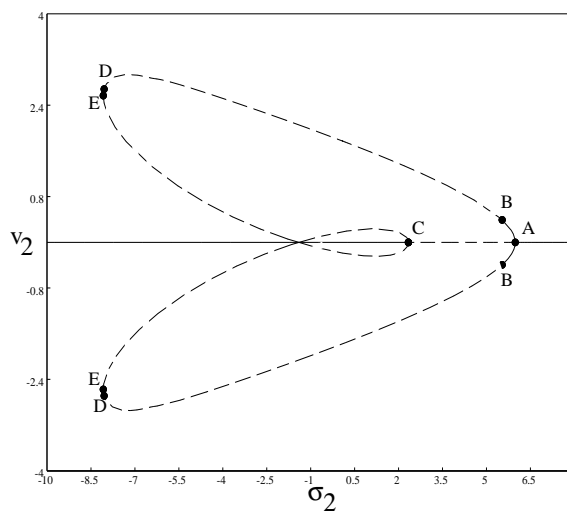


FIGURE 16. The stability diagram of system (4.1) in the (σ_2, v_2) -plane for $c_2 < 0$ close to the stability boundary.

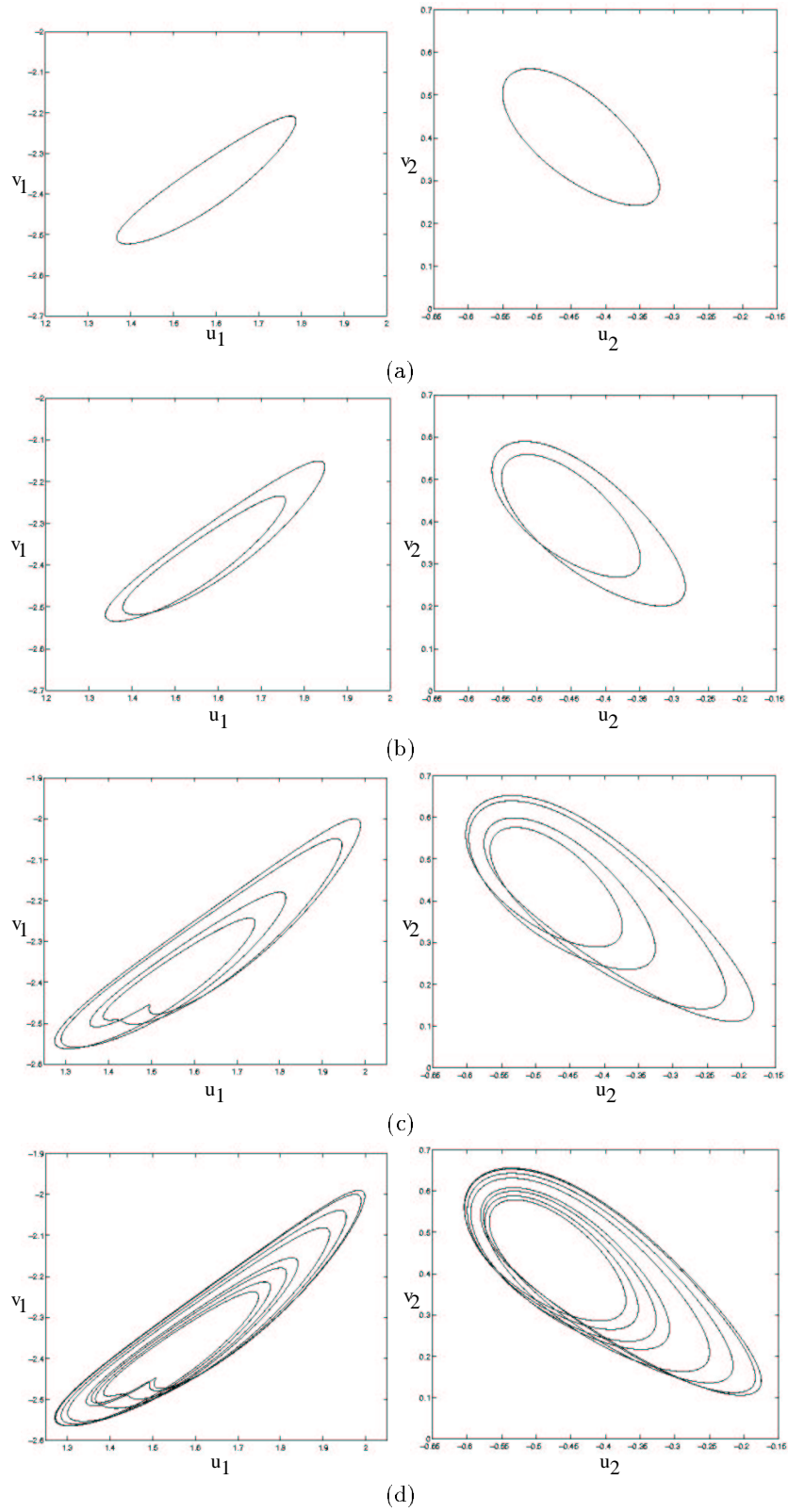


FIGURE 17. The sequence of period doubling bifurcations. The phase-portraits in the (u_1, v_1) -plane and (u_2, v_2) -plane for (a) $\sigma_2 = 5.42$, (b) $\sigma_2 = 5.4$, (c) $\sigma_2 = 5.344$, and (d) $\sigma_2 = 5.341$

In Figure 15 we fixed $\sigma_1 < 4\frac{k_2}{c_2}$, a close to $2k_1$ and $c_2 < 0$ ($a = 2.1$, $\sigma_1 = -8$, and $c_2 = -1$). The bifurcations of the semi-trivial solution are similar to the case where a is taken far away from the stability boundary (compare Figure 12 and Figure 16).

In Figure 16, the semi-trivial solution branches at point A, and then at point C. When the semi-trivial solution branches at point A, a stable non-trivial solution bifurcates and then this non-trivial solution undergoes a Hopf bifurcation at point B. We point out that a fixed point and a periodic solution in the averaged system correspond to a periodic and quasi-periodic solution, respectively, in the original, time dependent system. A supercritical Hopf bifurcation occurs at point B for $\sigma_2 = 5.5371$ and at point D for $\sigma_2 = -8.051$. Again, a saddle-node bifurcation occurs at point E for $\sigma_2 = -8.0797$. We find a stable periodic orbit for all values of σ_2 in the interval $5.4119 < \sigma_2 < 5.5371$. As σ_2 is decreased, period doubling of the stable periodic solution is observed, see Figure 17. There is an infinite number of such period doubling bifurcations, until the value $\sigma_2^* = 5.2505$ is reached. The values of σ_2 with $\sigma_2^* < \sigma_2 < 5.3195$ produce a strange attractor.

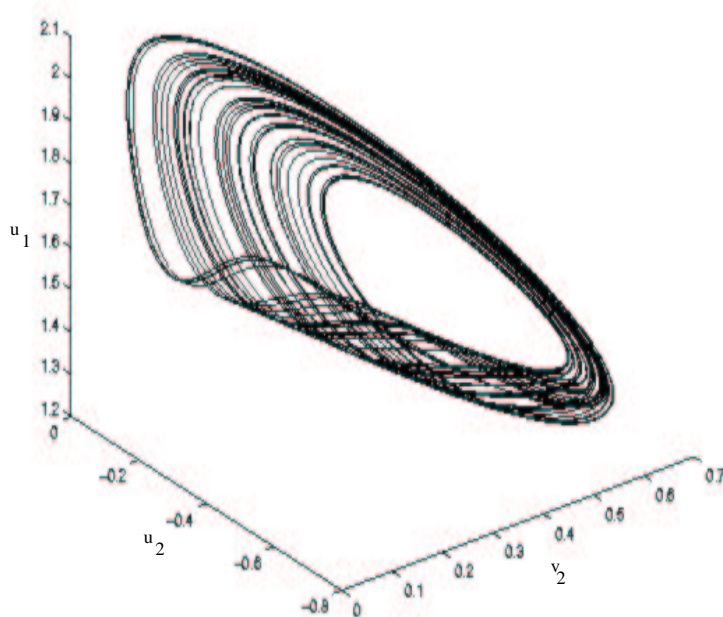


FIGURE 18. The strange attractor of the averaged system (2.5). The phase-portraits in the (u_2, v_2, u_1) -space for $c_2 < 0$ at the value $\sigma_2 = 5.3$.

To know whether the strange attractor is chaotic or not, we have calculated the Lyapunov exponents of system (4.1). Any system containing at least one positive Lyapunov exponent is defined to be chaotic, with the

magnitude of the exponent reflecting the time scale on which system become unpredictable (Wolf, Swift, Swinney, and Vastano [13]).

We find that the Lyapunov spectra of system (4.1) corresponding to parameter values above are $\lambda_1 = 0.8411$, $\lambda_2 = -0.3864$, $\lambda_3 = -0.1596$, and $\lambda_4 = -0.2858$, so that the orbits displayed in Figure 18 are chaotic. We have found that for other values of $c_1 > 0$, $c_2 < 0$, k_1 and k_2 the same type of scenario occurs i.e. periodic solutions which after a series of periodic-doublings lead to a strange attractor with one positive and three negative Lyapunov exponents.

The Lyapunov spectrum is closely related to the fractal dimension of the associated strange attractor. We find that the Kaplan-Yorke dimension of the strange attractor for $\sigma_2 = 5.3$ is 2.29.

7. CONCLUSION

An autoparametric system of the form (1.1), with the conditions stated in equation (2.1), has at most five semi-trivial solutions, which come in pairs and are symmetric with respect to $(0, 0)$. We have studied one semi-trivial solution, which is stable as a solution of (3.1), and considered its stability in the full system. The dependence of the stability of this solution on the forcing and the detunings is pictured in Figure 3 and 4. We find that there can exist at most one stable non-trivial periodic solution. By studying the bifurcations from the semi-trivial solution, we also find in some cases Hopf bifurcations, leading to quasi-periodic solutions. Also, we have observed cascades of period-doublings, leading to chaotic solutions. The fact that these chaotic solutions arise in the averaged system implies that chaotic dynamics is a prominent feature in the original system.

8. ACKNOWLEDGEMENTS

The authors wish to thank Prof. A. Tondl for formulating the problem. Thanks also to Prof. F. Verhulst for many suggestions and discussions during the execution of the research and for reading the manuscript. We thank L. van Veen for numerically calculating Lyapunov exponents and J.M. Tuwankotta for assistance in using the program. The research was conducted in the department of Mathematics of the University of Utrecht.

REFERENCES

- [1] R. Svoboda, A. Tondl, and F. Verhulst, Autoparametric Resonance by Coupling of Linear and Nonlinear Systems, *J. Non-linear Mechanics*. 29 (1994) 225-232.
- [2] A. Tondl, M. Ruijgrok, F. Verhulst, and R. Nabergoj, *Autoparametric Resonance in Mechanical Systems*, Cambridge University Press, New York, 2000.
- [3] M. Ruijgrok, *Studies in Parametric and Autoparametric Resonance*, Ph.D. Thesis, Universiteit Utrecht, 1995.
- [4] S.S. Oueini, C. Chin, and A.H. Nayfeh, Response of Two Quadratically Coupled Oscillators to a Principal Parametric Excitation, *to Appear J. of Vibration and Control*.

- [5] W. Tien, N.S. Namachchivaya, and A.K. Bajaj, Non-Linear Dynamics of a Shallow Arch under Periodic Excitation-I. 1:2 Internal Resonance, *Int. J. Non-Linear Mechanics*, 29 (1994) 349-366.
- [6] A.K. Bajaj, S.I. Chang, and J.M. Johnson, Amplitude Modulated Dynamics of a Resonantly Excited Autoparametric Two Degree-of-Freedom System, *Nonlinear Dynamics*, 5 (1994) 433-457.
- [7] B. Banerjee, and A.K. Bajaj, Amplitude Modulated Chaos in Two Degree-of-Freedom Systems with Quadratic Nonlinearities, *Acta Mechanica*, 124 (1997) 131-154.
- [8] W. Tien, N.S. Namachchivaya, and N. Malhotra, Non-Linear Dynamics of a Shallow Arch under Periodic Excitation-II. 1:1 Internal Resonance, *Int. J. Non-Linear Mechanics*, 29 (1994) 367-386.
- [9] Z. Feng, and P. Sethna, Global Bifurcation and Chaos in Parametrically Forced Systems with one-one Resonance, *Dyn.Stability Syst.*, 5 (1990) 201-225.
- [10] J.A. Sanders, and F. Verhulst, *Averaging Methods in Nonlinear Dynamical System*, Appl.math. Sciences 59, Springer-Verlag, New York, 1985.
- [11] Y.A. Kuznetsov, *Elements of Applied Bifurcation Theory*, Second Edition, Springer, New York, 1997.
- [12] S. Wiggins, *Global Bifurcation and Chaos*, Applied Mathematical Science 73, Springer-Verlag, New York, 1988.
- [13] A. Wolf, J.B. Swift, H.L. Swinney, and J.A. Vastano, Determining Lyapunov Exponent from a Time Series, *Physica*. 16D (1985) 285-317.